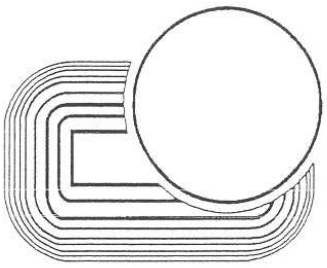

REACTION-DIFFUSION PROCESSES: APPLICATION TO THE MORPHOGENESIS OF AMMONOID ORNAMENTATION

Øyvind HAMMER & Hugo BUCHER

HAMMER O. & BUCHER H. 1999. Reaction-diffusion processes: application to the morphogenesis of ammonoid ornamentation. [Processus de réaction-diffusion: application à la morphogenèse de l'ornementation des ammonites]. GEOBIOS, **32, 6**: 841-852. Villeurbanne, le 31.12.1999.

Manuscrit déposé le 23.11.1998; accepté définitivement le 08.03.1999.

ABSTRACT - Ammonoid ribs, tubercles, keels and other ornamental features are organized in a great diversity of patterns. From the viewpoint of developmental biology, these patterns can only be understood as the product of a dynamical system controlled by genes but also dependent upon biochemical and mechanical processes. Here, an attempt is made to view the development of ammonoid ornamentation in the light of reaction-diffusion systems, though it is emphasized that diffusion of biochemical morphogens is only one of several possible interpretations of this class of theoretical models. Also, morphogenetical gradients and threshold functions are presented as partial explanations for some specific ornamental patterns.

KEYWORDS: AMMONITES, RIBS, DEVELOPMENT, REACTION-DIFFUSION, GRADIENTS, THRESHOLD DIFFUSION.

RÉSUMÉ - Les côtes, tubercules, carènes et autres éléments de l'ornementation des ammonites représentent une grande diversité de motifs. Du point de vue de la biologie du développement, ces motifs sont conçus comme le produit d'un système dynamique contrôlé par les gènes, mais aussi comme dépendants de processus biochimiques et mécaniques. Dans ce travail, le développement de l'ornementation des ammonites est modélisé par des systèmes de type réaction-diffusion, bien que la diffusion de morphogènes biochimiques ne soit qu'une des interprétations possibles parmi cette famille de modèles théoriques. Les gradients morphogénétiques et les fonctions de seuillage sont également utilisés pour rendre compte de certains motifs ornementaux particuliers.

MOTS-CLÉS: AMMONITES, CÔTES, DÉVELOPPEMENT, RÉACTION-DIFFUSION, GRADIENT, SEUIL DE DIFFUSION.

INTRODUCTION

Ammonoids have left a detailed fossil record, showing rapid evolution and high degree of morphological differentiation. Their phylogeny has been intensively studied. Also, the accretionary mode of growth of their shell makes it possible to reconstruct the ontogeny of the hard parts of individual specimens. All this makes ammonoids ideal for the study of relationships between ontogeny and phylogeny.

Developmental biology has shown that the genetic material does not contain a constructional "drawing" or blue-print for the final form. Rather, the genes code for the developmental processes, that is the rules that each cell should follow, given its own state and the state of its surroundings at any given time. In this way, the form builds itself "epigenetically", self-organizing into a functional and differentiated whole. It is in such terms we must try to understand the ontogenetical formation of ammonoid ornamentation: as a dynamical system where cells act locally in time and space, dependent upon the local biochemical and mechanical state, but ultimately under genetic control. It is upon this integrated system where genotype and phenotype are interconnected, that evolution acts.

A theory for the formation of ammonoid ribs was proposed by Checa (1995), based on the existence of microsculptures in well-preserved specimens. Checa explained these structures as the result of compressional folding in a flexible periostracum prior to calcification. In his model, there is little need for differentiation along the shell-secreting edge in order to produce the observed ribbing patterns. Bifurcating ribs form automatically as a result of the presumably periodical muscular contraction of the periostracum and soft body. While the evidence from microsculptures is strong and should not be taken lightly, there are problems with this model which should be considered, and which makes it worthwhile to keep other, partially competing models in mind as well. Some of these problems were noted by Bucher (1997), including

the existence of asymmetrical secondary ribs that connect to different primaries on each lateral side (this could only happen if the compression took place over a very long distance, spanning at least two primaries), as well as the occurrence of microsculptures in non-ornamented ammonoids. Also, there are problems in connection with complicated ornamentation, though some of these were addressed by Checa (1995). Discontinuous ribs, papillate ribs, spiral ribs, well-defined bifurcation zones, tubercles, spines, keels, multiple secondary ribs connected to a single point on the spaced-out primaries and looped ribs, all stand basically unexplained by the contraction model and are in part incompatible with it. For example, spines would have to form either in the non-mineralized zone before the retraction of the periostracum, in which case they would be soft and easily deformable, and would point in any direction after the retraction, or far behind the aperture after retraction, in which case the periostracum would have to be impossibly stretched from a basically flat sheet up into the spine.

The existence of microfolds in many non-ribbed mollusks speaks against using these structures as evidence for retractional macrofolding in ribbed forms. Tensional and more rarely compressional microfolds can be observed on the abrasion -resistant, green-brown periostracum of the living, smooth-shelled *Anodonta*. These may result either from the differential rate of periostracum secretion around the aperture or from the tension of the periostracum by the underlying outer prismatic layer as it is being secreted, or from the combination of both. The lenght of these microfolds never exceeds that of the millimetric growth increments which are delimited by the fringed, upturned adoral margin of the periostracal segments. This implies that the periostracum was not flexible over a long distance as proposed by Checa (1995). The processes of growth and mineralization in a mollusk shell are well capable of producing both tensional and compressional stresses in the periostracum (Skalak et al. 1997), and the latter could produce microfolds sub-parallel to the growing edge. Formation of compressional microfolds do therefore not necessarily require retraction of the periostracum. We rather suggest that the periostracum was formed in the shape of the final shell, also in ribbed forms, as normal for mollusks. The microfolds must be understood as the result of stresses generated by the differential growth of the periostracum related to the shape of the aperture and also perhaps from the later underlying calcification of the outer prismatic layer.

Interestingly, all ammonoid shells studied by Checa (1995, p. 866) are reported to have an irredescent appearance, which means that the nacreous composition of the shell is likely to be unalterned. Therefore, what has been illustated may correspond to microfolds affecting the nacreous layer, not those that may potentially occur on an outer prismatic layer as a calcified image of the internal side of the periostracum. If microfolds occurring on actual outer prismatic layer are very likely to reflect the underneath topography of the periostracum, microfolds occuring in the nacreous layer have a completely different significance and inevitably exclude any influence from the periostracum. As aragonitic ammonoid material frequently lacks the outer prismatic layer, distinction of microfolds of the outer primatic layer from those of the nacreous layer should be substantiated by preliminary ultrastructural investigations of the shell layers (see also Landman & Lane 1997).

Here, we go into some detail regarding the "reaction-diffusion" type of model briefly suggested for ammonoid ornamentation by Savazzi (1990) and Bucher (1997). This is a class of models that propose a specific pattern-forming system consisting of local biochemical interactions, forming a "prepattern" that would in turn control the local formation of ribs.

REACTION-DIFFUSION SYSTEMS

Ammonoid shell ornamentation includes spiral (longitudinal) strigation, transversal ribs, tubercles and keels. Following the work on mollusk pigmentation by Meinhardt & Klingler (1987) and Meinhardt (1995), the emergence of such structures can be modelled using reaction-diffusion systems acting in the linear growth zone. Savazzi (1990) mentions reaction-diffusion models in connection with mollusk sculpture (including ammonoid ribs), and Seilacher (1972) notes that mollusk pigmentation and sculpture seem to be controlled by a common morphogenetical mechanism, "the nature of which has still to be found out". He also extends the case to ammonoid aptychi, and brachiopods. His "divaricate" patterns have been modelled with cellular automata (Waddington & Cowe 1969) and using reaction-diffusion systems (Meinhardt 1995). Bucher (1997) also argues for a reaction-diffusion type patterning of ammonoid ribs.

Reaction-diffusion models for biological pattern formation, as introduced by Turing (1952), postulate the existence of one or more biochemical signalling factors, diffusing in tissue and reacting with each other through nonlinear kinetics. Depending on the reaction terms and the diffusion coefficients, such systems can show "self-organization" into ordered and polarized patterns from an initial random state. The concentration distributions then form a pre-

pattern which controls growth of some type of tissue. Reaction-diffusion models offer one simple biochemical explanation for the differentiation of initially equivalent cells into complex but ordered structures. It must be emphasized, however, that even if the reaction-diffusion model remains a powerful paradigm for pattern formation, reaction-diffusion has not yet been proved to be an important element in a large number of different developmental situations. For a number of developmental systems however, a reaction-diffusion-like process remains the best explanation. For a particularly well-documented example, see Noramly & Morgan (1998).

Still, it is not yet known whether diffusion is really an important factor in morphogenesis, and this has led to some confusion regarding reaction-diffusion models. It is more sensible to adopt a generalized "reaction-diffusion" model, where the signalling is not necessarily due to diffusion of physical molecules, but may happen through direct cell-to-cell communication by chemical or even mechanical (Odell et al. 1981) means. These different mechanisms can in fact be described by similar mathematical equations (Hammer 1998), forming a general model where the basic idea is pattern formation through local interactions including lateral inhibition and induction. Such mechanisms have been firmly demonstrated in developmental biology (Gilbert 1997). Abstract cellular automata models, that often do not try to model any specific biological process, fall under the same umbrella. For general reviews on reaction-diffusion models in developmental biology, the reader is referred to Meinhardt (1982) and Edelstein-Keshet (1988).

The following reaction-diffusion model is due to Meinhardt (1982) [see Hammer (1998) for another interpretation of the discretized version of this equation, where diffusion is not assumed]:

$$\partial a / \partial t = s(a^2 / b + b_a) - r_a a + D_a \nabla^2 a \qquad (1)$$
$$\partial b / \partial t = s a^2 - r_b b + b_b + D_b \nabla^2 b$$

The substance with concentration a is called the activator, and b is the *inhibitor*. The quadratic term sa^2/b models a situation where the activator is a catalyst for its own production. This may be due to some direct or indirect second-order biochemical autocatalytical reaction of the kind that is ubiquitous in gene regulation networks (for example, involving a dimeric enzyme inducing production of more enzyme), or a positive feedback loop with a mitogen inducing proliferation of more mitogen-producing cells. Also, the reaction is slowed down by the substance b; sb_a is the "basic activator production", $-r_a a$ is the decay term for the activator. The terms for the inhibitor b are similar, but its production is dependent on a in a nonlinear fashion.

Some degree of activator saturation is a reasonable addition to the model:

$$\partial a / \partial t = s(a^2 / b(1 + s_a a^2) + b_a) - r_a a + D_a \nabla^2 a$$

This set of equations is not meant to be more than a convenient model for theoretical analysis; the essential elements being a self-enhancing, localized activator signal coupled to an inhibitor which is propagating faster. Similar behaviour is shown by systems without a direct inhibitor, but with a "substrate" that is being depleted as the activator concentration increases.

For one-dimensional systems, the Laplace operators in equation (1) reduce to ordinary second derivatives. We use a simple difference method to approximate the solution numerically. The domain $X=[0,L]$ is partitioned by selecting a set $\{x_0=0, x_1, x_2, ..., x_{N-1}, x_N=L\}$ of $N+1$ points. For any $n \in \{0, 1, ...,N-1\}$, the spacing $x_{n+1}-x_n$ will be denoted h. The values of a and b are then sought at the grid points, so that $a_n \approx a(x_n)$.

The spatial second derivatives are approximated by discrete differences on this grid. Likewise, the time axis is discretized with a constant time increment Δt, so that $t_k=k\Delta t$.

$$(a^{k+1}{}_n - a^k{}_n) / \Delta t = F(a^k{}_n, b^k{}_n) + D_a(a^k{}_{n-1} - 2a^k{}_n + a^k{}_{n+1}) / h^2$$
$$(b^{k+1}{}_n - b^k{}_n) / \Delta t = G(a^k{}_n, b^k{}_n) + D_b(b^k{}_{n-1} - 2b^k{}_n + b^k{}_{n+1}) / h^2$$

These algebraic equations can be solved for $a^{k+1}{}_n$ and $b^{k+1}{}_n$, giving values for a and b at time $k+1$ explicitly as a function of the values at time step k. Δt is set to 1 (dimensionless unit). A pseudorandom distribution at time 0 is specified as the initial condition.

Cyclic boundary conditions impose the assumption that the concentration "wraps around" such that $a(0)=a(L)$. The interval $[0,L]$ can then be viewed as a circle. Cyclic boundary conditions are appropriate for many biological simulations in circular or cylindrical domains. In some of the simulations below, only the domain from the umbilical seam to the venter is simulated, and zero derivatives are then specified as boundary conditions.

SPIRAL RIBS (STRIGATION)

In the activator-inhibitor model, assume that the activator diffuses much more slowly than the

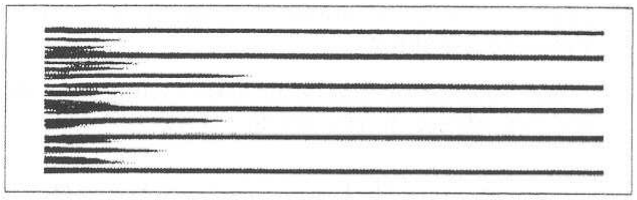

FIGURE 1 - Emergence of a stable pattern of strigation normal to the growing edge. Activator-inhibitor model, b_a=0, b_b=0, s=r_a=0.004, r_b=0.005, D_a=0.001, D_b=0.18, sa=0. A 100 cell grid was used, and run for 8000 time steps. In all figures, darker shading indicates higher activator concentration. *Emergence d'un motif stable de strigation perpendiculaire à la marge de croissance. Modèle activateur-inhibiteur* b_a=0, b_b=0, s=r_a=0.004, r_b=0.005, D_a=0.001, D_b=0.18, sa=0. *Modèle construit avec une grille de 100 cellules et évoluant sur 8000 incréments de temps. Dans toutes les figures, l'intensité du gris augmente avec la concentration de l'activateur.*

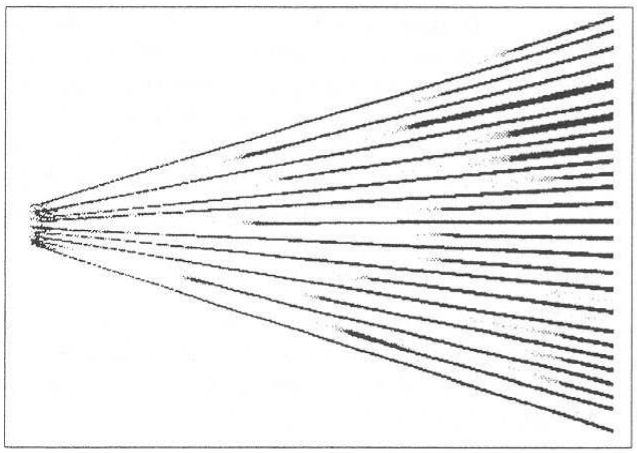

FIGURE 2 - Formation and insertion of striae in a growing domain. Activator-inhibitor model, b_a=0.1, b_b=0.001, s=r_a=0.004, r_b=0.005, D_a=0.001, D_b=0.28, sa=0. A 100 cell grid was used, and run for 20000 time steps. *Formation et insertion de stries dans un domaine de taille croissante. Modèle activateur-inhibiteur,* b_a=0.1, b_b=0.001, s=r_a=0.004, r_b=0.005, D_a=0.001, D_b=0.28, sa=0. *Modèle construit avec une grille de 100 cellules et évoluant sur 20000 incréments de temps.*

inhibitor (D_a<<D_b), for example because of a higher molecular weight. An initial random distribution of morphogens will then be *unstable,* since in any location where the activator concentration is slightly elevated, activator production is increased by autocatalysis, further increasing the concentration. Because the activator diffusion is comparatively slow, the activated zone will stay small and localized.

The inhibitor diffuses rapidly however, and despite its high production rate the local concentration will therefore not become sufficient to stop the formation of the activator peak. But the high level of inhibitor around the peak will have another effect: it will prevent other peaks from forming in the neighbourhood. The result can be the emergence of a stable, spaced pattern of activator peaks.

Spiral ribs are formed when the one-dimensional reaction-diffusion system produces such a stable spacing pattern. From a random initial distribution of morphogens, a pattern of spaced stripes emerges (Fig. 1). This may act as a pre-pattern to control rib growth. Longitudinal striae like this are less common in cephalopods than in other mollusks and in brachiopods, but they are seen in many Paleozoic ammonoids (especially *Goniatitina*), in the Triassic Flemingitidae, Sturiidae, Cladiscitidae and Joannitidae (all *Ceratitina*). Among the Ammonitina, the Liassic *Amaltheus pseudamaltheus* is one of the few Jurassic species with well developed strigation.

In a growing domain, as in the growth zone of a logarithmically coiled shell, ribs parallell with the direction of growth will be further and further spaced apart until the influence of the inhibitor gets sufficiently low for the insertion of new ribs (Fig. 2). Insertion of new ribs may or may not happen, depending on the parameters. For example, a low basic activator production b_a will prevent new ribs from emerging. In ammonoids a constant number of ribs during ontogeny is the normal mode. In this case, it is also possible that the morphogenetic process ceased early in ontogeny, thus fixing the pattern (Meinhardt 1995).

TRANSVERSAL RIBS: TEMPORALLY OR SPATIALLY CONTROLLED?

Below, oscillating reaction-diffusion systems will be described as a possible model for the development of transversal ammonoid ribs. Such a system would constitute an endogenous clock, giving rise to new ribs with constant time intervals (but note that this "clock" would be an emergent property of the self-organizing shell secretion system, and not a specific, localized entity). A discussion of the evidence for such a clocklike formation of ribs is therefore in place. For a review of ammonoid growth rates, see also Bucher et al. (1996).

One must be careful when using ribs as a growth rate indicator. Crowding of ribs near the aperture has been interpreted as showing retarded growth in adult ammonoids, but such crowding does not occur in all ammonoids. In perisphinctids, rib spacing rather increases at maturity, and such late transformation may be the result of special growth programmes that are switched on at maturity (Bucher et al. 1996). If we assume that the parameters in the reaction-diffusion system remain constant during the juvenile stage, the frequency of oscillation per time unit will also be constant, and rib density will be a reliable indicator of relative speed of growth. The assumption of constant oscillation frequency during ontogeny can only be checked using techniques that can give absolute growth rates. The isotopic paleotemperature measurements of Jordan & Stahl (1971) indicate that the

number of whorls per year in *Quenstedtoceras* and *Staufenia* is relatively constant at 0.25-0.4 (but see the discussion in Bucher et al. 1996). Commonly, the number of ribs per whorl is also relatively constant within each individual (Bayer 1977; see also Checa 1987), and these two observations together seem to indicate a fairly constant number of ribs per time unit. The assumption of a constant rib number per whorl may hold best for serpenticones however, and only within a single growth stage.

Let us analyze what constancy of rib number per whorl implies about growth rate under the assumption of constant oscillation frequency. Call the number of ribs per whorl N. The angular increment between successive ribs is then $\varphi=2\pi/N$. Measured in angular units per time, the growth rate is then a constant $g_\varphi=\varphi/T_0$, where T_0 is the assumed constant rib periodicity (inverse of frequency).

However, in a logarithmically coiling shell, a constant angular increment corresponds to an exponentially increasing growth distance. The total angle of revolution is $\Phi=\varphi t/T_0$, and the radius r of the shell at time t is $r=r_0e^{k\Phi}$ where k is related to the whorl expansion rate W (Raup 1966) by

$$K = ln\ W/2\pi$$

The growth distance (in units of length) between successive ribs is then

$$D = \varphi r = \varphi r_0 e^{k\,\varphi t/T_0}$$

(see also a similar but more complex derivation based on the Raup parameterization in Checa & Padilla 1990).

The absolute growth rate is therefore exponential as a function of time. Note that this is the growth rate measured in units of *length*. But due to the special properties of the exponential function, the growth rate is also exponential in units of surface area and in units of volume.

The commonly observed crowding of ribs per unit angle over ontogeny (e.g. Checa 1987) would then give a growth curve with a more logistic (sigmoidal) shape.

However, the assumptions underlying these calculations have been made on a less than firm basis. It should be noted that the rate of formation of septa in the *Nautilus* shell steadily decreases over ontogeny (Ward 1985), even though their angular increment remains nearly the same. This means that the angular growth rate (degrees per time unit) is decreasing, even though the linear growth rate (millimeters per time unit) may be stable or increasing due to larger radius. This raises a problem regarding the assumption above of constant number of whorls formed per time unit.

Another interesting consequence of this observation is that the initiation of new septa is not controlled by a temporal, clocklike mechanism, but rather by the advancement of the growing shell edge. When the distance between the latest septum and the aperture exceeds a threshold defined by a certain constant angle, a new septum is formed, regardless of the time since the last formation. This would render septa useless for studies of growth rates, as in claims about lunar cycles of septum formation with possibilities for determining ancient lunar orbital periods (Kahn & Pompea 1978).

This may prompt the question of the validity of postulating an endogenous clock as the control for rib formation. Might not the cyclicity of rib formation be controlled by a distance sensor rather than a timer, initiating a new rib whenever the angular distance to the previous rib is sufficiently large? The animal could sense the existence of a rib on the inside of the shell at a distance from the aperture. This signal would have to be propagated through soft tissue, since calcified shell is an impossible medium for the transportation of biochemical lateral inhibitors. However, the patterns of rib spacing after shell damage seem to indicate that the initiation of ribs was controlled temporally and by signalling from other areas of the growing edge, rather than by sensing the distance to previous ribs (Savazzi 1990, fig. 5). The same conclusion was reached by Doguzhaeva (1982) (but see the reply of Landman 1983). Dommergues (1988) explicitly supports using ribs as growth rate indicators, but he does this by showing correlation between septal and costal distances, which may be a questionable approach since both can be controlled by a third, not time correlated mechanism. The issue of constant frequency of rib (and septum) formation was also discussed by Checa (1987). Jordan & Stahl (1971) proposed a constant frequency of septum formation on the basis of their isotopic temperature measurements, but using data from only one whorl.

As a general observation, the common decreasing distances of septa and ribs the end of ontogeny speaks against a distance sensor for rib and septum spacing in ammonoids, leaving an endogenous or environmentally induced clocklike pulse as a more probable explanation. However, it must never be forgotten that developmental parameters may change over ontogeny (Bayer 1977; Bucher et al. 1996). Bayer (1977) provides one of the most thorough investigations on ammonoid growth rates. Using information from injured and aberrant individuals, he claims that the production of septa was controlled temporally, with a fixed frequency, independent from the growth of the conch. When an ammonoid was injured, the growth of the body chamber slowed down. In these cases, the septa are

crowded together, indicating that they were still inserted with a fixed period. Ribs are also claimed to be produced at a fixed rate, but their spacing is more strictly regulated and constrained by the mechanical properties of the mantle, in particular its maximal bending angle.

Indeed, the connections and dependencies between linear, angular and volumetric growth rates, linear and angular costal increments, linear and angular septal increments, linear and angular distances between growth lamellae, and linear, angular and volumetric size, are so complex and confusing that no general consensus seems to have been reached among researchers. More studies relating all these parameters to absolute time using isotopic or other methods are needed. It would not be surprising if septal and costal increments turn out to be controlled by a complex regulatory system where both temporal and spatial information is important.

RIBS SUB-PARALLELL TO THE GROWING EDGE

For certain parameter ranges, reaction-diffusion systems will oscillate. Given that ammonoid ribs are initiated at regular time intervals (which is by no means established, as discussed in the previous section), such an oscillating system can explain the occurrence of ribs which are more or less parallell with the growing edge. This mode is the normal one for ammonoids. Simple ribs like in figure 3 are seen in *Caloceras* and many other genera. It is now clear that non-linear, biochemical reaction systems are responsible for many biological rhythms (Aronson et al. 1994), thus strengthening this theory.

If the shell is injured, the regeneration can give clues to the growth process. If the geometrical rib pattern were "hard-coded" in the genotype, we would expect a regenerated area of shell with the same orientation of ribs as in the normal shell. If, however, a locally controlled oscillating process is responsible for the ribbing, we should find ribs parallell with the healing growth edge, which may be oblique with respect to the normal growth edge. This is exactly what is found in several studies of regenerated ammonoid shells (Bayer 1970; Landman & Waage 1986; Bond & Saunders 1989 for similar observations regarding growth lamellae). Savazzi (1990) provides particularly clear examples. He concludes that ammonoid ribs can be modelled as the result of periodic inflation of the mantle margin, and that sculpture and colour patterns are programmed independently from shell shape. The pigmentation patterns on *Nautilus* shells show the same mode of striping parallell to the wounded edge as strikingly illustrated by Ward (1987, fig. 3.28).

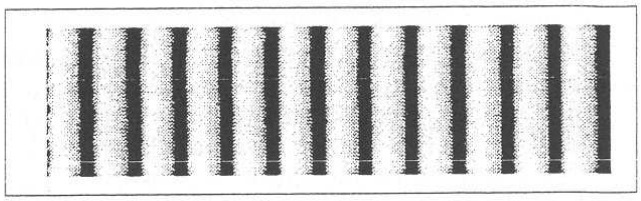

FIGURE 3 - Oscillations in an activator-substrate model are synchronized across the growing edge because of diffusion. b_a=0.04, b_b=0.1, s=r_a=0.2, r_b=0.002, D_a=0.3, D_b=0.35, sa=0.1. A 100 cell grid was used, and run for 8000 time steps. *Synchronisation des oscillations le long de la marge de croissance dans un modèle activateur-substrat avec diffusion* b_a=0.04, b_b=0.1, s=r_a=0.2, r_b=0.002, D_a=0.3, D_b=0.35, sa=0.1. *Modèle construit avec une grille de 100 cellules et évoluant sur 8000 incréments de temps.*

BIFURCATIONS AND GRADIENTS

Ammonoids often show rib patterns where the number of ribs per whorl is larger on the ventral than on the umbilical side. This may cause separate insertion of secondary ventral ribs, or lead to the formation of bifurcations. Such patterns are helpful in understanding the formation of ribs. For example, environmental fluctuations, which would influence all parts of the growth zone with equal frequency, must have played a secondary role at most in the timing of rib onsets. Similarly, an internal oscillator with a single frequency ("master clock") is not a sufficient explanation.

Meinhardt 1995 modelled bifurcations in the pigmentation of *Nautilus* with an oscillating reaction-diffusion system where one of the parameters increased linearly from umbilicus to venter. This causes the frequency of oscillation to increase along the growth zone. A typical experiment with such a morphogenetical gradient (Wolpert 1969) on the basic activator production is shown in figure 4. Several interesting phenomena can be seen. The frequency at the top (venter) is about 1.7 times the frequency at the bottom (umbilicus). Since this factor is not an integer, the ribs will tend to drift in and out of phase. When a primary and a secondary (ventral) rib are nearly in phase, they may blend together because of activator diffusion, forming a bifurcation. But when the ribs are out of phase, the secondary rib will end blindly, because the distance to the nearest neighbour rib is too large for coalescence. The resulting somewhat irregular fluctuation between bifurcation and truncation is a familiar pattern in ammonoids, as illustrated for example by dactylioceratids (Guex 1973) and haloritids (Bucher 1997). This observation strengthens the theory that rib formation is a locally determined, emergent phenomenon, like most processes known from developmental biology, rather than the result of a strictly controlled growth program that might produce more stable and repeating patterns.

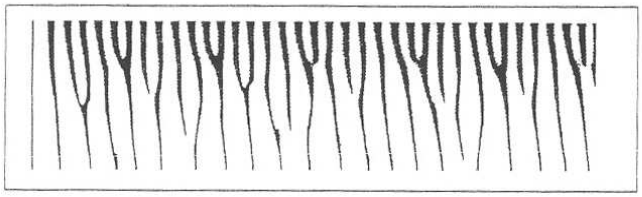

FIGURE 4 - Bifurcations can form in an oscillating activator-inhibitor model when the basic activator production is under the control of a morphogenetic gradient. b_a varies from 0.02 (bottom) to 0.08 (top), b_b=0.00001, s=r_a=0.1, r_b=0.01, D_a=0.4, D_b=0.2, sa=0.1. A 100 cell grid was used, and run for 8000 time steps. The activator was thresholded at a=0.15 for plotting purposes. *Formation de bifurcations dans un modèle activateur-inhibiteur oscillant quand la production de l'activateur est contrôlée par un gradient morphogénétique.* b_a *varie de 0.02 (bas) à 0.08 (haut),* b_b=0.00001, s=r_a=0.1, r_b=0.01, D_a=0.4, D_b=0.2, sa=0.1. *Modèle construit avec une grille de 100 cellules et évoluant sur 8000 incréments de temps. L'activateur est seuillé pour* a=0.15 *pour la représentation graphique.*

Since a logarithmically coiled shell has a linear growth rate which is increasing from umbilicus to venter, it is possible that the logarithmic growth and the formation of branching ribs are under control of similar, possibly interconnected or even identical morphogenetic gradients. In accordance with this theory, straight-shelled heteromorph ammonoids (baculitids) show at most very weak rib branching, and the ventral and dorsal rib count are almost equal. More compelling evidence is given by certain heteromorphs that periodically switch between straight and curved shell growth. Branching of ribs may then occur in the curves, where the growth gradient along the aperture is steep, but not on the straight sections. An example is the Cenomanian *Hamites* (Wright & Kennedy 1981, p. 110).

It is unlikely that the morphogenetic gradient responsible for the umbilico-ventral oscillation frequency gradient is maintained by continued diffusion from a ventral organizer, as in the antero-posterior Bicoid gradient of *Drosophila* (see Gilbert 1997, p. 543-556, for an overview). Because of constant diffusion rates, the gradient would not scale with the increase in size during growth. A more likely model is that the gradient was established early in ontogeny possibly at the protoconch stage, and its positional information gave positional values to the cells along the growth edge. These values would be remembered using similar memory mechanisms as are being used to explain similar processes in e.g. *Drosophila* (permanent activation of homeotic selector genes by positive feedback mechanisms or by changes in chromatin structure), even when the original morphogenetic gradient was removed.

Checa & Westermann (1989) reported that the growth lines in ammonoids with bifurcating ribs show angular conformation with the ribs. This would mean that the growth would have to pause at a rib "stem" while an intercalary wedge is secreted between two branches. Such a complicated growth mechanism is difficult to explain. A reaction-diffusion process of the simple type described here would have to take place somewhat anteriorly of the edge where the growth lines are secreted, and would have to form a prepattern that controls both the ribbing and the migration of growth loci. In nautiloids with highly oblique ribs (Seilacher 1972), angular conformation between the growing edge and the ribs is impossible, however. Similar oblique ornamentation is found in ammonoids (e.g. the Triassic *Catenohalorites*). Also, Checa (1995) noted exceptions to the general rule of conformation between growth lines and ribs, and Bucher (1997) uses aspects of rib morphology to argue against the "segmental growth" theory. In most forms with radial ribs, partial unconformity is best seen at branching points. This may have been overlooked by many workers.

THE PROBLEM OF DIFFUSION RATES

So far, we have not addressed a serious objection to this whole theory, namely the constant and low rates of diffusion likely to be found in nature. Consider now the example given in figure 4. We have used D_a=0.4, Δt=1 and h=1 in dimensionless units, but let us look at what the real diffusion coefficient would have to be to produce the same result with sensible values for time and distance. Assuming, rather arbitrarily, that the figure represents a time span of 1 year, the 8000 time steps imply Δt=3942 seconds, or about one hour. Note that this is just the computational time step in our numerical procedure, which is based on the simplifying assumption of continuous secretion. No connection with any periodicity of secretion is implied or needed. Assuming a distance from the umbilical seam to the venter of 10 cm, we get the following equation derived from equation (1):

$$D_a \Delta t / h^2 = D_a \cdot 3942 / (10/100)^2 = 0.4\ s/cm^2$$

$$\text{giving } D_a = 1.01 \cdot 10^{-6}\ cm^2/s$$

Interestingly, this value is right in the range expected for a diffusible signal molecule. Edelstein-Keshet (1988) quotes a value of D=1.9810^{-5} cm^2/s for an oxygen molecule in water at 25 degrees Celsius. A small signal molecule would probably have a higher mass than this, therefore diffusing slower. However, a very large ammonoid with a distance from the umbilical seam to the venter of 50 cm would need a diffusion rate of D_a=2.54 10^{-5} cm^2/s, if all the other parameters from the example above are kept constant. This is a too high diffusion rate for a signal molecule of any complexity. For mammalian skin patterns, Murray (1981) sugges-

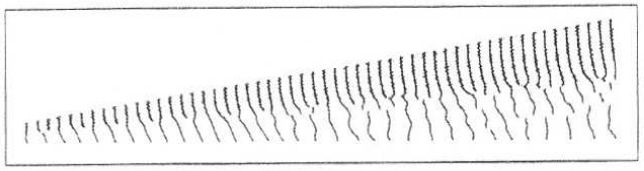

FIGURE 5 - Branching and intercalation of ribs in a growing geometry, with cell size h varying from 1 to 6. Ribs are continuous in early stages, but break up as the structure grows. A similar development is seen in *Margarijuvavites*. b_a varies from 0.01 (bottom) to 0.09 (top) as in figure 4, b_b=0.00001, s=r_a=0.05, r_b=0.01, D_a=0.25, D_b=0.2, sa=0.0. A 100 cell grid was used, and run for 20000 time steps. *Branchement et intercalation de côtes sur un support géométrique augmentant de taille, avec une taille de cellules h variant de 1 à 6. Les côtes sont continues dans les premiers stades, puis se fragmentent avec l'augmentation de taille du support. Un développement similaire est connu chez* Margarijuvavites. b_a *varie de 0.01 (bas) à 0.09 (haut) comme dans la figure 4,* b_b=*0.00001,* s=r_a=*0.05,* r_b=*0.01,* D_a=*0.25,* D_b=*0.2,* sa=*0.0. Modèle construit avec une grille de 100 cellules et évoluant sur 20000 incréments de temps.*

ted that the prepattern forms at an early embryonic stage, when the dimensions are very small.

It therefore seems that we must postulate signalling mechanisms relying on signals which can propagate a little faster than by pure diffusion. This is unproblematical. Any slight convection, streaming of fluids in tissue, would suffice to transport the signalling molecules at the necessary speed and without changing the resulting patterns (at least as long as the convection is not unduly biased in one direction). Some mechanical mediator is also possible, for example the propagation of local folding or inflation of membranes with a certain stiffness in the soft tissues of the shell-secreting mantle (as in the pneu model of Savazzi 1990), or propagation of folding in the periostracum (Checa 1995). And finally, local cell-cell interactions could provide the signal (Hammer 1998).

Another problem is the presumed constant diffusion rates during growth. We have seen in the case of spiral strigation that the patterns emerging from the reaction-diffusion simulations change as the geometry is expanding. Similar effects also occur in the case of oscillating patterns. As the simulated shell is growing, the ribs tend to become fragmented (Fig. 5). This is not a frequent case in real ammonoids, where the rib patterns seem to scale with size. However, at least two very interesting exceptions known from the Triassic are the "randomly distributed blunt clavate nodes" of *Margarijuvavites* (Tozer 1994, p. 240) and the "papillate" ornamentation of *Eutomoceras* (Silberling & Nichols 1982, p. 35). In *Margarijuvavites*, fine and regularly spaced ribs of upper flanks break up into the so-called random nodes on inner flanks (compare Figs 5,6). In *Eutomoceras*, ribs are continuous in early growth stages, but the ornamentation breaks up into to discontinuous weak ribs on the outer whorls (Fig. 7).

To account for the more normal case where ribs stay continuous over ontogeny, one must assume increased speed of signal propagation as the structure grows, due to e.g. increasing metabolic rate, or because of a mechanical propagation method that scales with size. For some parameters however, the mode of branching is remarkably robust as the geometry is expanding. In figure 8, the length of the growth zone is expanded by a factor of 6, while all other parameters are kept constant.

We will continue to use diffusion models, but keeping in mind that other signalling mechanisms may have been involved as well. The main principles of local, autocatalytical activation, lateral inhibition and possible chemical oscillation stay untouched.

EVIDENCE FOR MORPHOGENETIC SWITCHES

The simulations above show *diversipartite* branching of ribs, meaning that the bifurcations take

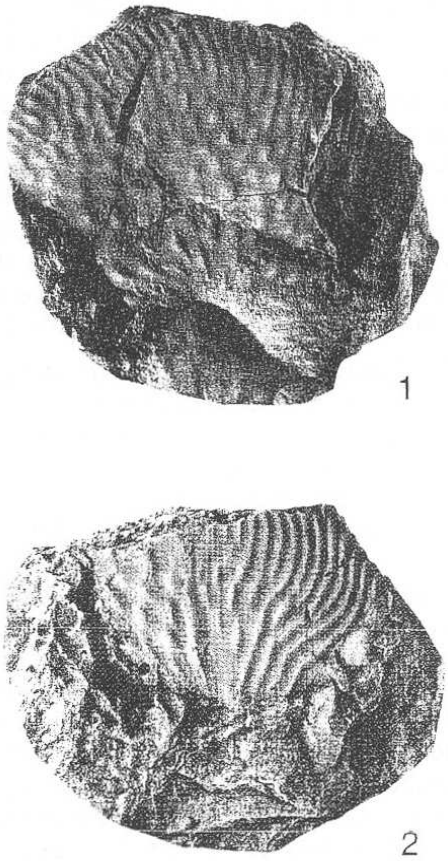

FIGURE 6 - *Margarijuvavites carlottensis* (WHITEAVES), from Tozer 1994. 1. Specimen showing the transition from the ventral regular ribbing to the lateral nodes [x 1]. 2. Specimen showing the ontenetic transition from regular ribbing to the node pattern [x 1]. *1. Spécimen montrant la transition entre la costulation ventrale normale et les nodosités latérales [x 1]. 2 Spécimen montrant la transition ontogénétique entre la costulation normale et le motif en nodosités latérales [x 1].*

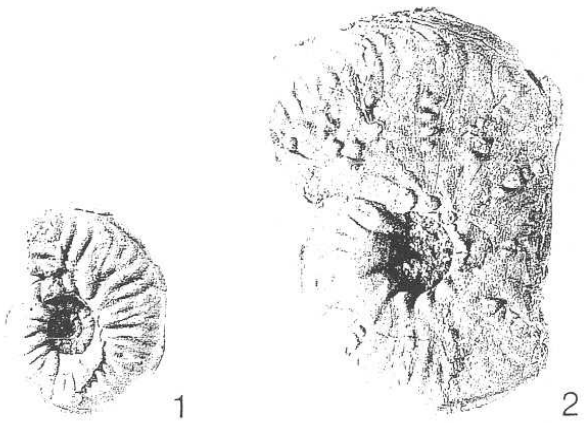

FIGURE 7 - *Eutomoceras dunni* SMITH. **1.** Early ontogenetic stage with continuous, regular ribbing [x 1]. **2.** Later ontogenetic stage showing the transition between ribs and papillate nodes [x 1]. *1. Stade ontogénétique précoce avec costulation normale et continue [x 1]. 2. Stade ontogénétique plus tardif montrant la transition entre les côtes et les nodosités papillées [x 1].*

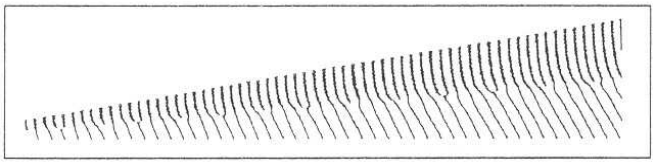

FIGURE 8 - Branching and intercalation of ribs in a growing geometry, with cell size h varying from 1 to 6. While the branching pattern is stable, the ribs get more oblique. b_a varies from 0.01 (bottom) to 0.09 (top) as in figure 4, b_b=0.0001, s=r_a=0.05, r_b=0.01, D_a=0.4, D_b=0.2, sa=0.4. A 100 cell grid was used, and run for 20000 time steps. *Branchement et intercalation des côtes sur un support géométrique augmentant de taille, avec une taille de cellules h variant de 1 à 6. Bien que le motif de branchement reste stable, les côtes deviennent plus obliques.* b_a *varie de 0.01 (bas) à 0.09 (haut) comme dans la figure 4,* b_b=*0.0001,* s=r_a=*0.05,* r_b=*0.01,* D_a=*0.4,* D_b=*0.2,* sa=*0.4. Modèle construit avec une grille de 100 cellules et évoluant sur 20000 incréments de temps.*

place at irregular positions. In contrast, many ammonoids show *monoschizotomous* branching, meaning that the bifurcations take place at a single, well defined position. Also, there are di- and trischizotomous forms. These different modes of rib branching have taxonomical value.

Schizotomous bifurcation can be explained by postulating abrupt changes in the umbilico-ventral morphogenetic gradient at certain positions. This may be caused by a thresholding transfer function which translates an underlying smooth gradient into a discontinuous field. A similar mechanism is used to explain segmentation in arthropods like *Drosophila* (Gilbert 1997, ch. 14). Thresholding of a smooth gradient can be a natural consequence of basic biochemical processes (Edelstein-Keshet 1988; Lewis et al. 1977). Given a smooth gradient of a morphogen with concentration s, the equation

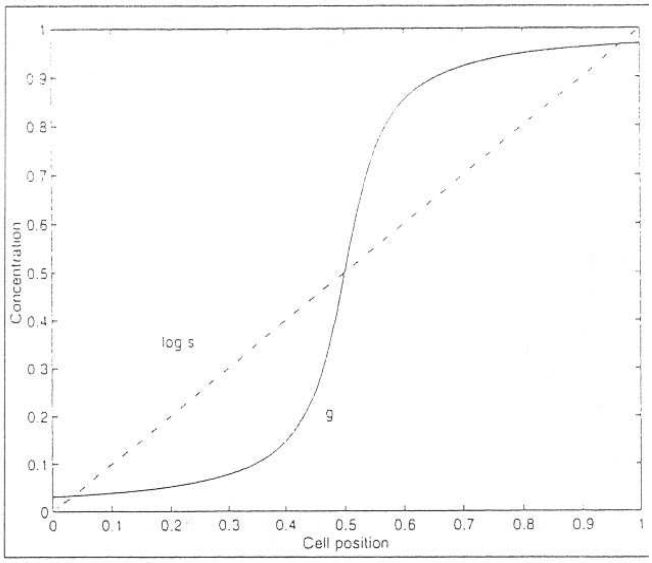

FIGURE 9 - A bimodal response to a loglinear morphogenetic gradient, with a rapid transient. Redrawn after Edelstein-Keshet 1988. *Réponse bimodale à un gradient morphogénétique loglinéaire avec une transition rapide. Redessiné d'après Edelstein-Keshet 1988.*

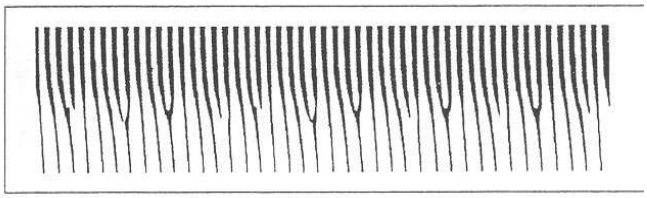

FIGURE 10 - A rapid transition in the parameter gradient will cause the secondary ribs to form at a constant position. Activator-inhibitor model. b_a varies from 0.01 (bottom) to 0.09 (top), b_b =0.0001, s=r_a=0.05, r_b=0.01, D_a=0.3, D_b=0.1, sa=0.5. A 100 cell grid was used, and run for 16000 time steps. The activator was thresholded at a=0.16 for plotting purposes. *Une transition rapide dans le gradient conditionne un positionnement constant des côtes secondaires. Modèle activateur-inhibiteur.* b_a *varie de 0.01 (bas) à 0.09 (haut),* b_b=*0.0001,* s=r_a=*0.05,* r_b=*0.01,* D_a=*0.3,* D_b=*0.1,* sa=*0.5. Modèle construit avec une grille de 100 cellules et évoluant sur 16000 incréments de temps. L'activateur est seuillé à* a=0.16 *pour la représentation graphique.*

below will translate this field into a bimodal distribution of another substance with concentration g:

$$dg/dt = k_1 s - k_2 g + Kg^2/(k_n + g^2)$$

The term $k_1 s$ models a production dependent on s, $-k_2 g$ expresses degradation of the substance over time, and the final fraction models an autocatalytic sigmoidal positive feedback effect. The steady state of this equation as a function of s is shown in figure 9.

Such a bimodal concentration distribution may then be postulated to control some parameter (like basic activator production) in the morphogenetic field along the ammonoid growth zone. This can cause a more or less constant and low frequency of ribbing in the umbilical zone, rapidly increasing to a high frequency ventrally. The

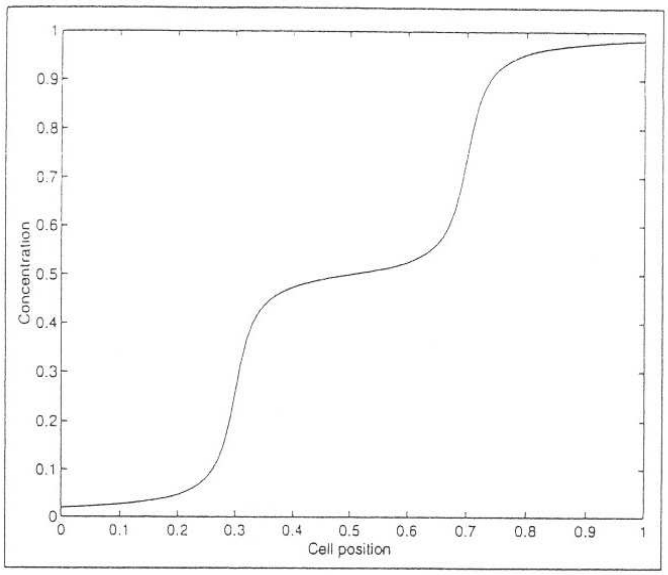

FIGURE 11 - The superposition of two gradient bimodal systems makes a stepped concentration distribution along the growth edge. *La superposition de deux systèmes bimodaux de gradients morphogénétiques conduit à une forte concentration le long de la marge de croissance.*

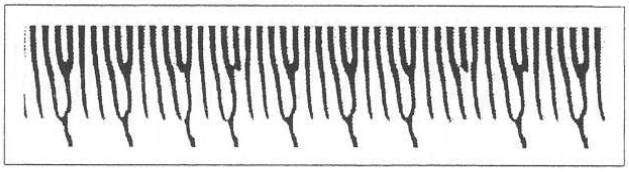

FIGURE 12 - A superposition of two step-like responses to an underlying smooth gradient produces a bischizotomous branching pattern. Activator-inhibitor model. b_a varies from 0.0001 (bottom) to 0.08 (top), with two transients. b_b=0.0005, s=r_a=0.03, r_b=0.01, D_a=0.15, D_b=0.15, sa=0.6. A 100 cell grid was used, and run for 20000 time steps. The activator was thresholded at a=0.2 for plotting purposes. *La superposition de deux réponses seuillées à un gradient sous-jacent lisse génère un motif de branchement bischizotome. Modèle activateur-inhibiteur.* b_a *varie de 0.0001 (bas) to 0.08 (haut), avec deux transitions.* b_b=*0.0005,* s=r_a=*0.03,* r_b=*0.01,* D_a=*0.15,* D_b=*0.15,* sa=*0.6. Modèle construit avec une grille de 100 cellules et évoluant sur 20000 incrèments de temps. L'activateur est seuillé à* a=*0.2 pour la représentation graphique.*

result will be a well-defined, stable region of bifurcation and insertion of secondary ribs in the small transition zone (Fig. 10).

Once such a mechanism has evolved, simple duplication mutations may be enough to produce several such systems with somewhat different parameters. The superposition of their bimodal responses could cause several transition zones along the growth zone, explaining multischizotomous branching (Fig. 11). An attempt at simulating bischizotomous branching is shown in figure 12.

TUBERCLES

Many ammonoids have evenly spaced tubercles, and these tubercles are often placed at points of rib bifurcation. Simple models can explain both the placing of tubercles and their typical co-occurrence with bifurcations.

In morphological descriptions, the wording is often that the tubercles "give rise to" bifurcations. Actually, it is difficult to ascertain the causal sequence: whether the formation of tubercles initiates branching, or vice versa. A third possibility is that the two phenomena occur under the control of a third, simple mechanism - a morphogenetic switch. Such a model is proposed here. We take the schizotomous branching models from the last section as our point of departure.

The simplest model is that a tubercle forms when two conditions are met: that the rib growth factor is high (if not, tubercles might form between ribs, which is less common), and that the concentration of the graded morphogen falls within a certain range. Because of the rapid transition in the gradient, a small distance along the growth zone, near the bifurcation, will correspond to a large concentration range. The selectivity of the morphogen sensor of the tubercle forming system will therefore not have to be large. To further localize the tubercle, this system might in addition contain a lateral inhibition element that would constrain its lateral extent.

Mechanisms like these are well known in developmental biology. Thresholding of a morphogenetic gradient is now the standard explanation for the formation of segments in *Drosophila*. The antero-posterior gradient controls the emergence of localized, narrow and well defined features along the axis, in the same manner as in the tubercle model above. Though the actual network of interacting gene products is rather complex, the total behaviour of the system can be described with simple models (Gilbert 1997, ch. 14; Meinhardt 1994). Segments do not emerge directly in a self-organizing, two-morphogen system. This is

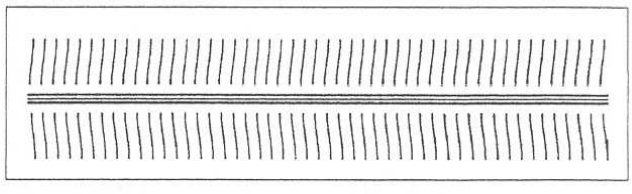

FIGURE 13 - A tricarinate keel pattern. High basic activator production in the centre of the domain creates a stable spacing pattern. Note the inhibition of ribs near the keel. b_a=0.05, but b_a=0.15 in the ventral region. b_b=0.00001, s=r_a=0.08, r_b=0.02, D_a=0.01, D_b=0.2, sa=0.3. A 100 cell grid was used, and run for 10000 time steps. The activator was thresholded at a=0.4 for plotting purposes. *Motif de carène tricarénée. Une forte production d'activateur au centre du domaine génère un motif à espacement stable. Noter l'inhibition des côtes au voisinage de la carène.* b_a=*0.05, mais* b_a=*0.15 dans la région ventrale.* b_b=*0.00001,* s=r_a=*0.08,* r_b=*0.02,* D_a=*0.01,* D_b=*0.2,* sa=*0.3. Modèle construit avec une grille de 100 cellules et évoluant sur 10000 incréments de temps. L'activateur est seuillé à* a=*0.4 pour la représentation graphique.*

not surprising - such elements, critical to the body plan, are likely to be more strictly controlled using hierarchical, combinatorial mechanisms.

MIXTURES OF STABLE AND OSCILLATING PATTERNS. KEELS

An interesting mode of growth in many ammonoids is combination of periodic and stable patterns in a single shell. The most common example is periodic ribbing with a stable keel on the venter. In such cases, the ribs often terminate before they reach the keel (e.g. *Pleuroceras*). This behaviour is easy to understand if a reaction-diffusion mechanism is responsible, because the level of inhibitor (or substrate depletion) around the keel would be high and stable, effectively suppressing the periodic ribbing. Guex (1967, 1968) clearly showed that a deep enough ventral injury may cause the deletion of the keel and its replacement by the lateral ribbing in the subsequent, repaired shell. The term "ornamental compensation" was then coined for this type of ornamental property. Bayer (1970) also observed aberrant individuals of a species that normally possesses ribs that terminate before they reach the keel. If the keel is absent, the ribs continue uninterrupted over the venter, indicating that the keel in normal specimens inhibited the formation of ribs, or at least that the keel and ribs were part of an interconnected, dynamical system.

A keel can be produced in a reaction-diffusion system if the basic activator production has a peak at the venter. If the peak is sufficiently broad, more than one stable stripe can form, making lateral "false keels". In figure 13, the typical tricarinate-bisulcate keel pattern of e.g. *Arietites* has been simulated in this way.

For some parameter ranges (high saturation in particular), the ribs may be able to connect with the keel, and this is also seen in some ammonoids. Another possible effect is that the oscillatory process that controls the ribs also influences the formation of the keel, resulting in a serrated keel as known from many species (Fig. 14).

CONCLUSION

We have here tried to speculate on ammonoid ornamentation in terms of development rather than function. This is an attempt at mechanistic rather than teleological explanation, bridging the gap between genes and morphology.

Though reaction-diffusion models should be regarded as formal, or even formalistic, conceptual frameworks for understanding development, we believe that they capture some of the essence of biological pattern formation. To interpret the diffusion term as diffusion of physical signal molecules may not be correct in all cases, but the important lesson from reaction-diffusion theory lays more in the idea of a dynamical and locally acting process of patterning, with some kind of lateral signalling.

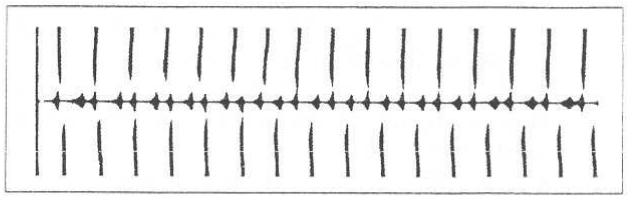

FIGURE 14 - Serrated keel pattern. High basic activator production in the centre of the domain creates a single keel which is influenced by the rib-forming oscillations. Ribs are inhibited near the keel. b_a=0.03, but b_a=0.3 at the keel. b_b=0.00001, s=r_a=0.08, r_b=0.01, D_a=0.18, D_b=0.4, sa=0.01. A 100 cell grid was used, and run for 8000 time steps. The activator was thresholded at a=0.15 for plotting purposes. *Motif de carène cordée. Une forte production d'activateur au centre du domaine génère une carène simple qui est affectée par les oscillations formant les côtes. Les côtes sont inhibées au voisinage de la carène.* b_a=*0.03, mais* b_a=*0.3 à l'emplacement de la carène.* b_b=*0.00001,* s=r_a=*0.08,* r_b=*0.01,* D_a=*0.18,* D_b=*0.4,* sa=*0.01. Modèle construit avec une grille de 100 cellules et évoluant sur 8000 incréments de temps. L'activateur est seuillé pour* a=*0.15 pour la représentation graphique.*

The mechanism for the formation of ammonoid ribs likely included a multitude of processes, both biochemical and mechanical. Hopefully, the developmental biologists working on recent mollusks will soon be able to constrain our speculations.

Acknowledgments - Ø. Hammer's contribution to this paper is part of a project in developmental paleobiology supported by the Research Council of Norway. This paper also benefited from stimulating discussions on ammonoid microsculptures with R. Chirat. Constructive reviews by G. Carbonnel and A. Schaaf also improved an earlier version of this work. E.T. Tozer provided illustrations of *Margarijuvavites*. Photographic illustrations of *Eutomoceras* were prepared by N. Podevigne.

REFERENCES

ARONSON B.D., JOHNSON K.A., LOROS J.J. & DUNLAP J.C. 1994 - Negative feedback defining a circadian clock: autoregulation of the clock gene frequency. *Science*, 263: 1578-1583.

BAYER U. 1970 - Anomalien bei Ammoniten des Aaleniums und Bajociums und ihre Beziehung zur Lebensweise. *Neues Jahrbuch für Geologie und Paläontologie, Abhandlungen*, 135: 19-41.

BAYER U. 1977 - Cephalopoden-Septen Teil 2: Regelmechanismen im Gehäuse- und Septenbau der Ammoniten. *Neues Jahrbuch für Geologie und Paläontologie, Abhandlungen*, 155: 162-215.

BOND P.N & SAUNDERS W.B. 1989 - Sublethal injury and shell repair in Upper Mississippian ammonoids. *Paleobiology*, 15: 414-428.

BUCHER H. 1997 - Caractères périodiques et mode de croissance des ammonites: comparaison avec les gastéropodes. *Geobios*, M.S. 20: 85-99.

BUCHER H., LANDMAN N.H., KLOFAK S.M. & GUEX J. 1996 - Mode and Rate of Growth in Ammonoids. *In* LANDMAN N.H., TANABE K. & DAVIS R.A. (eds), *Ammonoid Paleobiology. Topics in Geobiology,* 13: 407-461. Plenum Press, New York.

CHECA A. 1987 - Morphogenesis in ammonites - differences linked to growth pattern. *Lethaia,* 20: 141-148.

CHECA A. & WESTERMANN G.E.G. 1989 - Segmental growth in planulate ammonites. *Lethaia,* 22: 95-100.

CHECA A. & PADILLA A. 1990 - Length versus revolution angle in coiled shells. *Lethaia,* 23: 310.

CHECA A. 1995 - A model for the morphogenesis of ribs in ammonites inferred from associated microsculptures. *Palaeontology,* 37: 863-888.

DOGUZHAEVA L. 1982 - Rhythms of ammonoid shell secretion. *Lethaia,* 15: 385-394.

DOMMERGUES J.-L. 1988 - Can ribs and septa provide an alternative standard for age in ammonite ontogenetic studies? *Lethaia,* 21: 243-256.

EDELSTEIN-KESHET L. 1988 - *Mathematical models in Biology*. 586 p. McGraw-Hill, New York.

GILBERT S.F. 1997 - *Developmental Biology,* 918 p., Sinauer Associates, Inc. Publishers, Massachusetts.

GUEX J. 1967 - Contribution à l'étude des blessures chez les ammonites. *Bulletin de la Société vaudoise des Sciences naturelles*, 69/323.

GUEX J. 1968 -Sur deux conséquences particulières des traumatismes du manteau des ammonites. *Bulletin de la Société Vaudoise des Sciences Naturelles,* 70/328.

GUEX J. 1973 - Dimorphisme des Dactylioceratidae du Toarcien. *Eclogae geologicae Helvetiae*, 66: 545-583.

HAMMER Ø. 1998 - Diffusion and direct signaling models are numerically equivalent. *Journal of Theoretical Biology,* 192: 129-130.

JORDAN R. & STAHL W. 1971 - Isotopische Paläotemperatur-Bestimmungen an jurassischen Ammoniten und grundsätzliche Voraussetzungen für diese Methode. *Geologisches Jahrbuch,* 89: 33-62.

KAHN P. & POMPEA S. 1978 - *Nautilus* growth rhythms and dynamical evolution of the Earth-Moon system. *Nature,* 275: 606-611.

LANDMAN N.H. 1983 - Ammonoid growth rhythms. *Lethaia,* 16: 248.

LANDMAN N.H. & LANE J.A. 1997 - Foldlike irregularities on the shell surface of Late Cretaceous ammonoids. *American Museum Novitates,* 3197: 1-15.

LANDMAN N.H. & WAAGE K.M. 1986 - Shell abnormalities in scaphitid ammonites. *Lethaia,* 19: 211-224.

LEWIS J., SLACK J.M.W. & WOLPERT L. 1977 - Thresholds in development. *Journal of Theoretical Biology,* 65: 579-590.

MEINHARDT H. 1982 - *Models of Biological Pattern Formation*. Academic Press, London.

MEINHARDT H. 1994 - Biological pattern formation: new observations provide support for theoretical predictions. *Bioessays,* 16: 627-32.

MEINHARDT H. 1995 - *The Algorithmic Beauty of Sea Shells,* 204 p. Springer-Verlag, Berlin.

MEINHARDT H. & KLINGLER H. 1987 - A model for pattern formation on the shells of mollusks. *Journal of Theoretical Biology*, 126: 63-89.

MURRAY J.D. 1981 - A Prepattern formation mechanism for animal coat markings. *Journal of Theoretical Biology*, 88: 161-199.

NORAMLY S. & MORGAN B.A. 1998 - BMPs mediate lateral inhibition at successive stages in feather tract development. *Development,* 125, 19: 3775-3787.

ODELL G.M., OSTER G., ALBERCH P. & BURNSIDE B. 1981 - The mechanical basis of morphogenesis 1: epithelial folding and invagination. *Developmental Biology,* 85: 446-462.

RAUP D.M. 1966 - Geometric analysis of shell coiling: general problems. *Journal of Paleontology*, 40: 1178-1190.

SAVAZZI E. 1990 - Biological aspects of theoretical shell morphology. *Lethaia,* 23: 195-212.

SEILACHER A. 1972 - Divaricate patterns in pelecypod shells. *Lethaia,* 5: 325-343.

SILBERLING N.J. & NICHOLS K.M. 1982 - Middle Triassic molluscan fossils of biostratigraphic significance from the Humboldt Range, northwestern Nevada. *Geological Survey Professional Paper,* 1207.

SKALAK R., FARROW D.A. & HOGER A. 1997 - Kinematics of surface growth. *Journal of Mathematical Biology,* 35: 869-907.

TOZER E.T. 1994 - Canadian Triassic ammonoid faunas. *Geological Survey of Canada Bulletin*, 467.

TURING A. 1952 - The chemical basis of morphogenesis. *Philosophical Transactions of the Royal Society of London,* 237: 37-72.

WADDINGTON C.H. & COWE J.R. 1969 - Computer simulation of a molluskan pigmentation pattern. *Journal of Theoretical Biology*, 25: 219-225.

WARD P.D. 1985 - Periodicity of chamber formation in chambered cephalopods: evidence from *Nautilus macromphalus* and *Nautilus pompilius*. *Paleobiology*, 11: 438-450.

WARD P.D. 1987 - *The Natural History of Nautilus,* 263 p., Allen & Unwin, Boston.

WOLPERT L. 1969 - Positional information and the spatial pattern for cellular differentiation. *Journal of Theoretical Biology,* 25: 1-47 p.

WRIGHT C.W. & KENNEDY W.J. 1981 - *The Ammonoidea of the Plenus Marls and the Middle Chalk*. Monograph of the Palaeontographical Society, London.

Ø. HAMMER
Paleontological Museum, University of Oslo
Sars gt. 1
0562 Oslo, Norway
e-mail: oyvind.hammer@notam.uio.no

H. BUCHER
CNRS ERS 2042, U.F.R. Sciences de la Terre
Université Claude-Bernard Lyon I
43 boulevard du 11 Novembre
F-69622 Villeurbanne cedex
e-mail: bucher@univ-lyon1.fr